# *Chapter@5*

## *Effect of diamine functionalized graphene oxide on polyurethane properties*

## 5.1 Introduction:

Segmented polyurethanes (SPUs) are versatile polymeric materials whose properties can be tailored by changing the nature and functionality of the precursor molecules. Polyurethanes (PUs) are widely used in foam, adhesive, coating and in biological fields due to its damping ability, elasticity, flexibility and biocompatible nature [Saha et al. (2008); Park et al. (2002); Qian et al. (2011)]. Mechanical responses of the polymeric materials can be enhanced by the incorporation of different types of fillers in the polymer matrix such as carbon nanotubes [Koerner et al. (2004)], Graphene [Kim et al. (2010)], nanoclays [Chen et al. (2000)], metal and its oxides [Bishop et al. (1992): Morones et al. (2005)] etc. Currently, graphene, allotropes of carbon, has drawn enormous attention in composite materials due to its unique properties such as exceptional electronic conductivity [Novoselov et al. (2004)], mechanical strength [Rao et al. (2009)], optical properties [Zhang et al. (2010)], thermal [Balandin et al. (2008)] and its biocompatibility [Kalbacova et al. (2010)]. These superior properties of graphene make it an excellent material for a wide range of applications [Yan et al. (2012)]. Graphene has a two-dimensional hexagonally orientated single-layer of carbon sheets and analogous to layered silicate nanoclay structure [Chen et al. (2008); Li et al. (2008)]. Better dispersion as well as reduction in the aggregation of graphene sheets in various polymer matrices is achieved through surface functionalizations. Agglomerations are restricted due to the presence of bulkier organic modifiers which can either be hydrophilic or hydrophobic in nature. The electronic structure of graphene containing compositess can be modified further either through the application of uniaxial strain as well as the chemical surface functionalizations [Ohta et al. (2006); Ni

et al. (2008)]. Modification may cause the decrease in the conductivity through the formation of defect and also in the presence of insulating groups which deteriorate the flow of the electron to help decreasing the conductivity but it enhances the other properties [Kim et al. (2013)]. Chemical modification of graphene through covalent grafting makes it an attractive material for a wide range of applications such as sensor and increase its solubility in various medium [Englert et al. (2011)]. Most frequently amino acids, polymers, amines of aliphatic or aromatic chains are used for surface functionalization [Kuilla et al. (2010)]. Stacking of the graphene oxide sheets have effectively minimized by the reaction of the diisocyante with hydroxyl and carboxyl groups presents in the graphene oxide [Zhang et al. (2009)].

This chapter consist the surface functionalization of graphene oxide with diamine having different length of alkyl moieties and evaluated its effect on the structure, morphology and various properties of polyurethane-graphene nanocomposites such as thermal, mechanical and biological uses to understand the effect of chain length of functionalization on the properties of nanocomposite. Prominent interaction between the modified graphene and polymer matrix is monitored through spectroscopic techniques. Self-assembly phenomenon has been studied from the nanometer dimension molecular sheet to micron size inhomogeneities which get facilitated in presence of chemically tagged modified graphene. Improvements in thermal and mechanical properties are observed in nanocomposites as compared to pure polymer. Biological behavior of pure polyurethane and its nanocomposites are observed using human breast cancer cell line. Controlling of sustained drug release from the polymer matrix is reported using those chemically tagged nanocomposites. Thus, a novel

material has been developed based on these biological responses as well as the controlled release of the loaded drug using chemically tagged graphene nanocomposites of polyurethanes.

## 5.2 Results and Discussion:

### 5.2.1 Functionalization of graphene oxide:

FTIR spectra of graphene oxide and modified graphene with a series of diamines (ethylene diamine, hexyl diamine and dodecane diamine) have been shown in (Figure 5.1 a). Appearance of the new peak in the range of 1576-1568 $cm^{-1}$ indicates the presence of the >C–N moiety in modified graphene oxides due to the insertion of the $–NH_2$ group in the epoxide carbon through nucleophilic substitution and confirms the formation of the amine modified graphene [Kim et al. (2013)]. Peak intensities at 2924 and 2845 $cm^{-1}$ reflect the asymmetric and symmetric vibration of the methylene group ($–CH_2–$) in the modified graphene which also supports the incorporation of respective alkyl chains into graphene ring [Wu et al. (2012)]. Enhanced intensities for longer chain lengths of the diamine modifier further indicate their presence attached with the graphene ring (functionalization with varying diamines) [Shim et al. (2012)]. UV-Visible spectra of graphene oxide and modified graphene are presented in (Figure 5.1b). Pure graphene oxide exhibits a prominent absorption peak at 235nm due to $\pi \rightarrow \pi^*$ transition of >C = C< bonds and a shoulder at 262nm for $n \rightarrow \pi^*$ transition for –COOH group [Innocenzi et al. (2009)]. The absorption band at 235nm has shifted to 254nm in modified graphene and this red shift in the absorption spectra indicates the enhancement of conjugation caused by simultaneous reduction process at the time of

surface functionalization and favorable interactions between modified moieties [Kim et al. (2013)]. Further, the shoulder peak in modified graphene also shows the red shift while the absorption intensities are weak due to reduction of >C=O group.

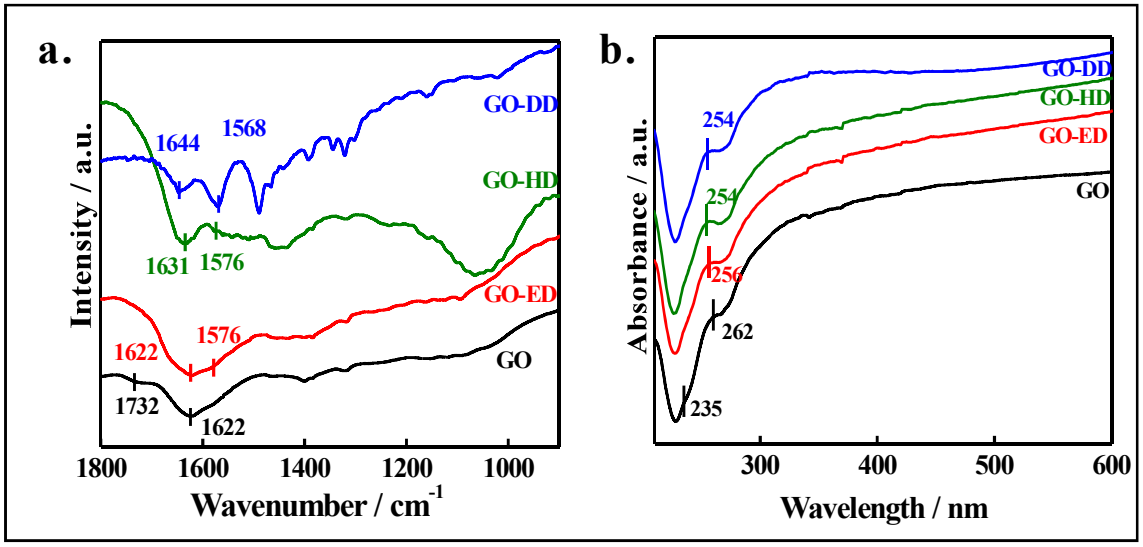


**Figure 5.1: (a)** FITR spectra of graphene oxide and diamine modified graphene oxide. **(b)** UV-visible spectra of graphene oxide and various diamine functionalized graphene oxide in solid state.

### 5.2.2 XRD and $^{1}$H-NMR of graphene oxide and modified graphene oxide:

XRD patterns of the graphene oxide and dimine modified graphene are shown in (Figure 5.2a). Graphene oxide exhibits a diffraction peak at $12.2^{0}$ with corresponding d-spacing of 0.74 nm while XRD peak shifting for functionalized graphene towards lower angle indicate the enhancement of intergallery d-spacing of graphene sheets due to insertion of the modifier chains [Ma et al. (2012)]. Bourlinos et al. (2003) reported the insertion of alkyl moiety from the reaction with epoxide in graphene oxide through surface functionalization [Bourlinos et al. (2003)]. Chemical tagging of diamine moiety

to graphene sheet are proved through $^{1}$H-NMR to understand the change in hydrogen environment and given in (Figure 5.2b). Appearance of a strong peak at δ=2.1 ppm in modified graphene (representing the methylene group) confirms the chemical tagging of diamine moiety to graphene sheet [Li et al. (2011)].

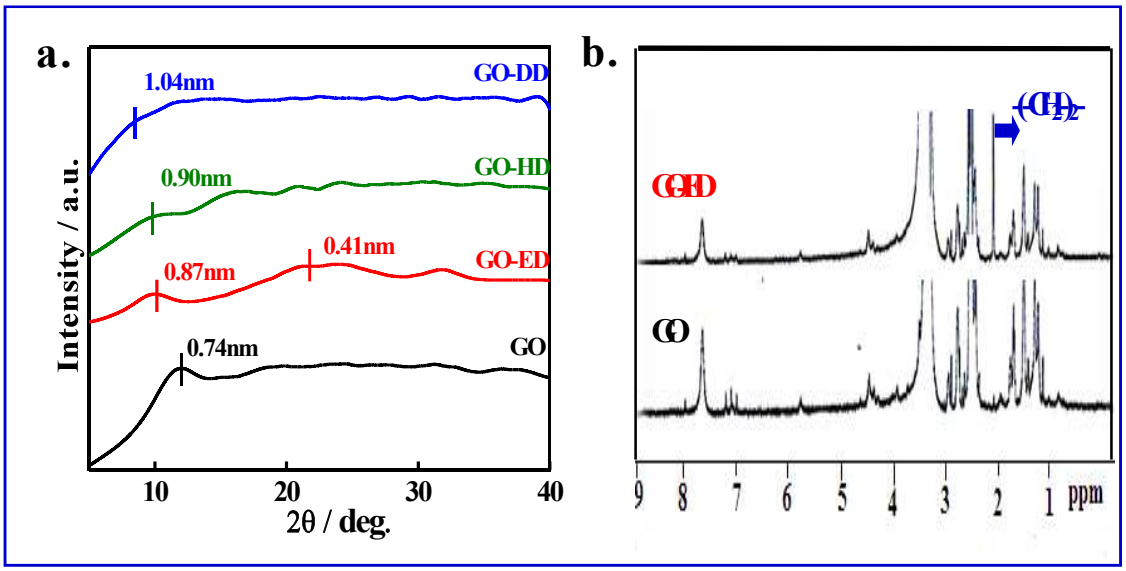


**Figure 5.2: (a)** X-ray diffraction pattern of graphene oxide and diamine functionalized graphene oxide and **(b)** Proton NMR spectra of graphene oxide and ethylene diamine modified graphene oxide.

### 5.2.3 Graphene tagged polyurethanes and interactions:

Varying lengths of diamines (ethyl, hexyl and dodecane diamine) tagged graphene oxides have been used as chain extenders to synthesize polyurethanes. $^{1}$H-NMR spectra of pure polyurethane and modified graphene tagged PU is shown in (Figure 5.3). Pure PU exhibits a peak at δ ~7.0 ppm arising from >N–H group in polymer chain [Mishra et al. (2010)]. However, an additional peak is observed at δ ~8.0 ppm in nanocomposites originated from the grafted >N–H moiety between modified graphene and prepolymer and thereby confirms the grafting of prepolymer chain with the

modified graphenes. Properties of nanocomposite material strongly depend upon the state of the filler dispersion into the matrix.

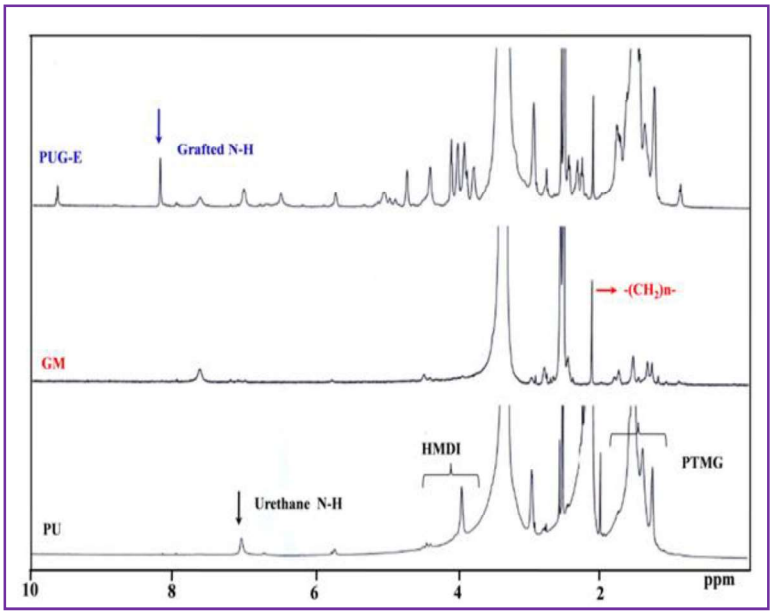


**Figure 5.3:** $^{1}$H-NMR spectra of pure PU and indicated nanocomposites with modified graphene.

Dispersion of the modified graphene in polymer matrix is presented in (Figure 5.4a).Nanocomposites having the smaller or larger chains of chemical tagging (ethylene diamine or dodecyl diamine) in graphene modification exhibit homogeneous dispersion. The cause of this good dispersion is explained through better interactions between modified graphene and polymer matrix.

Interaction between polymer matrix and modified graphene is verified through the FTIR spectra and gradual shifting of FTIR peaks of 3318, 3321, 3324 and 3327 $cm^{-1}$ for PU, PUG-E, PUG-H and PUG-D, respectively, for the >N−H stretching frequency of urethane linkages (Figure 5.4b) [Wang et al. (1983)]. Appearance of the absorption

band of >C=O group at 1683 $cm^{-1}$ in pure polymer indicates the presence of extensive H-bonding through urethane linkages in polymer chains [Williams et al. (2008)]. On contrary, suppression of this peak is noticed in nanocomposites while a peak at 1718 $cm^{-1}$ getting intense due to non hydrogen bonded >C=O stretching peak arising from the greater interaction between modified graphene and PU instead of interactions between urethane linkages alone in pure polymer [Patel et al. (2015)]**.** Moreover, pure polymer shows two UV absorption peak at 253 and 284nm arises from $\pi \rightarrow \pi^*$ and $n \rightarrow \pi^*$ transition, respectively (Figure 5.4c) [Chen et al. (2005)]. Significant red shifting of $n \rightarrow \pi^*$ transition (284→292nm) is observed in nanocomposites along with a minor shift of $\pi \rightarrow \pi^*$ transition (253→254nm) in all nanocomposites strongly indicative of the better interactive systems in nanocomposites (between the modified graphene with rest of PU chains). However, spectroscopic evidences of stronger interactions between the components support in turn the good dispersion of modified graphene in polymer matrix, prepared through in-situ method raising the expectation of better properties of nanocomposites as compared to pure polymer.

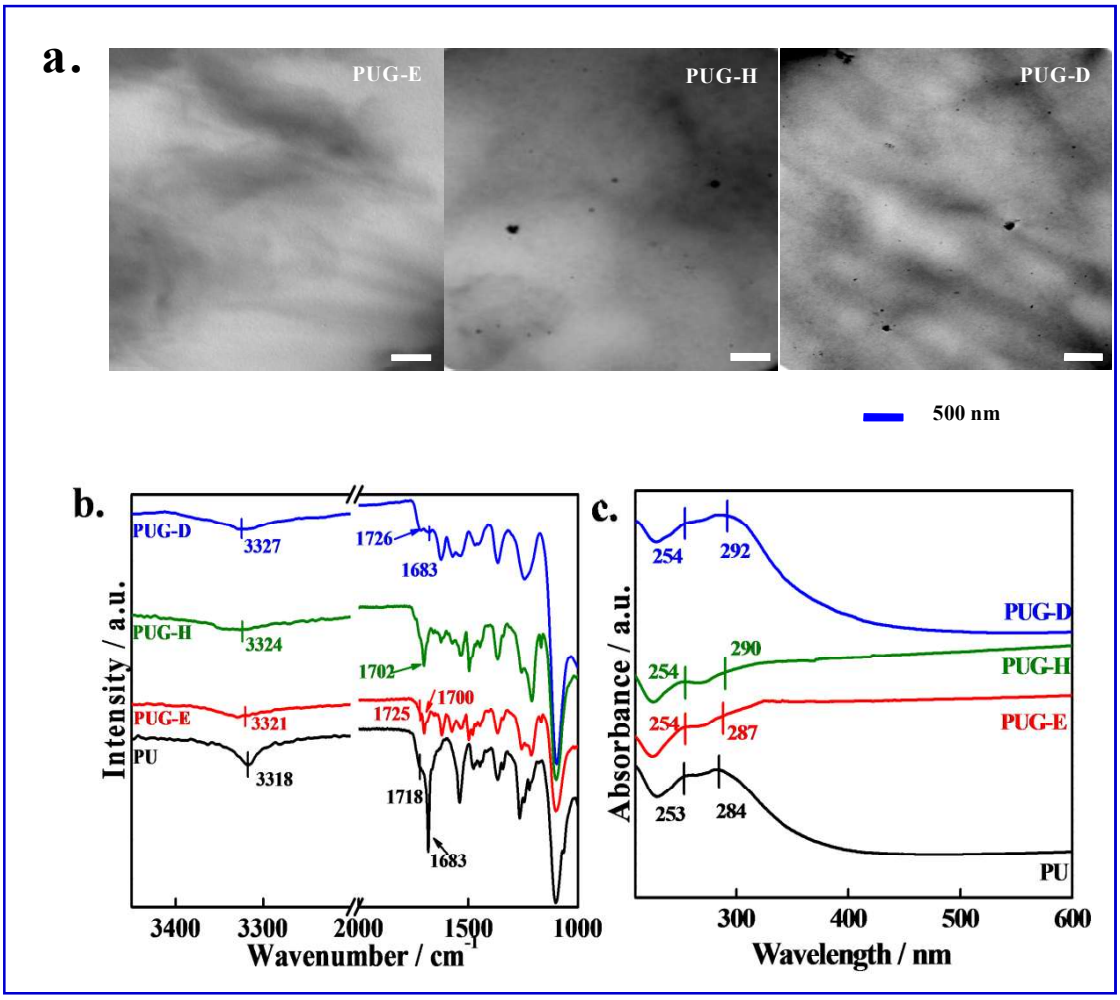


**Figure 5.4: (a)** Transmission electron micrographs of the indicated PU nanocomposites**. (b)** FTIR spectra of the pure PU and its indicated nanocomposites and **(c)** UV-vis pectrum of pure polymer and its indicated nanocomposites.

### 5.2.4 Morphology and structure:

Effect of diamine modified graphene on the morphology of polyurethane is studies by SEM measurement and given in (Figure 5.5a). Diamine modified graphene show the grain morphology indicating the crystalline nature whereas; nanocomposite exhibits the clothy appearance in their morphology suggesting the amorphous nature. Inhibition of crystallization of hard segment in nanocomposites is also verified through XRD measurement as evident from the absence or lower intense peak at 24.9$^{o}$ as opposed to

the intense peak position for pure PU at similar diffraction angle (Figure 5.5b). Similar reduction of crystallinity of thermoplastic PU in presence of graphene (not chemically tagged with PU) is reported in the literature [Nguyen et al. (2009)]. However, the stronger peaks at 23.6° for nanocomposite in comparison to pure PU support higher crystallinity of soft segment in line with DSC results.

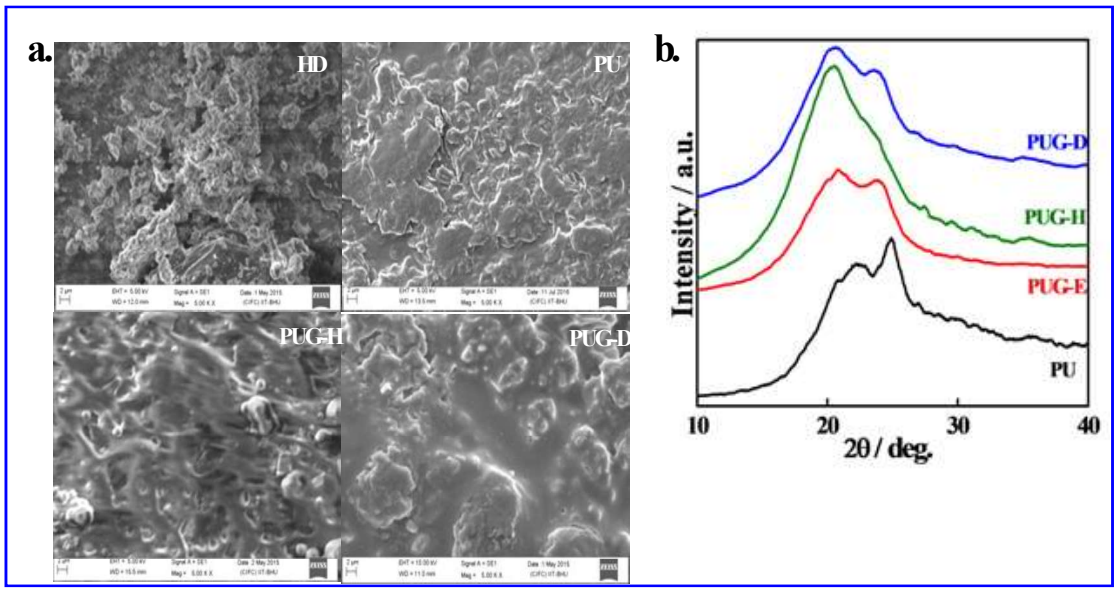


**Figure 5.5: (a)** SEM image of hexyl diamine modified graphene oxide, pure polyurethane and indicated nanocomposites and **(b)** XRD pattern of pure PU and its indicated nanocomposites.

### 5.2.5 Effect of modified graphene tagging on thermal stability and structure:

Thermal stability of the nanocomposites was checked through thermogravimetric measurements and the degradation temperatures were found to be 278, 291, 296 and 342°C for pure PU, PUG-E, PUG-H and PUG-D, respectively, showing significant thermal stability of the nanocomposites as compared to pure PU (Figure 5.6a). This is to mention that the temperature corresponding to the loss of 5 wt. % polymer was

considered as the degradation temperature. However, chemical modification of graphene grafted with PU protects the organic polymer from thermal degradation and longer chain length of modifier further increases the thermal stability through better dispersion. Pure PU and its nanocomposites exhibit two stages of degradation and relatively lower temperature weight loss is due to urethane linkages associated with hard segments of the polymer chain which are more sensitive towards heat followed by the degradation of soft segments of PU [Nair et al. (2001)]. The grafting of hyperbranched aromatic polyamide ring into graphene oxide was reported to have similar improvement in thermal stability in the literature and was presumably due to the elimination of oxygen moieties during reduction [Wu et al. (2012)]. The improvement in thermal stability of the diamine modified graphene oxide / polystyrene composites is reported by Ma et al. [Ma et al. (2012)]. However, this enhancement in the thermal stability is more prominent in PU nanocomposites having longer chain of diamine which facilitated the compatibility between the polymer matrix and modified graphene through greater interaction.

DSC thermograms of PU and its nanocomposites are presented in (Figure 5.5b) exhibiting a sharp endothermic peak in lower temperature region, corresponds to the melting temperature of the soft segments of the chains both for pure PU and its nanocomposites at 17.8, 18.1, 20.1 and 20.3 $^{o}$C for PU, PUG-E, PUG-H and PUG-D, respectively [Patel et al. (2015)]. Gradual increasing of this peak towards higher temperature region for nanocomposites with longer chain of modifier indicates greater interactions with modified graphene. Interestingly, high temperature melting peak of pure PU at 154 $^{o}$C, due to melting of hard segments of polymer, disappears in

nanocomposites indicating the absence of agglomerated hard segment in nanocomposites due to better interaction with modified graphene instead of strong interaction between exclusive urethane linkages to form hard segments in pure PU.

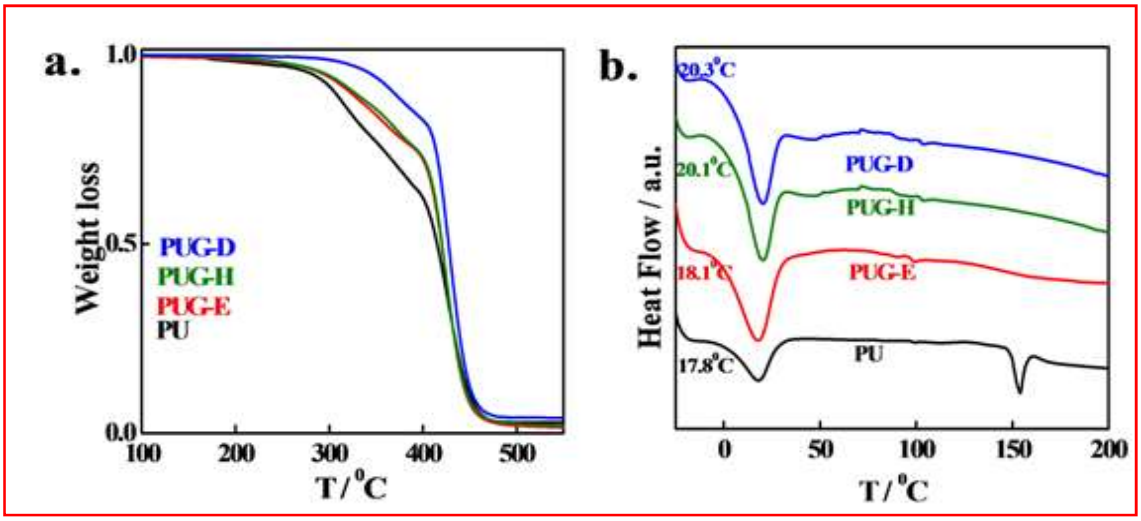


**Figure 5.6: (a)** TGA thermograms of the pure PU and its indicated nanocomposites **(b)** DSC thermograms of PU and indicated nanocomposites.

### 5.2.6 Mechanical responses - effect of graphene tagging:

Mechanical responses of composite materials are strongly correlated with the type and level of dispersion of filler in the polymer matrix. Stress-strain curves of pure PU and its nanocomposites under the uniaxial stretching are presented in (Figure 5.7a). Nanocomposites exhibit much higher toughness, as measured from the area under stress-strain curves, as compared to pure PU with the exception of dodecyl diamine functionalized graphene nanocomposite where there is considerable decrease of both the modulus and toughness with respect to pure PU for unknown reason (Figure 5.6b and c). Lower modulus of nanocomposites vis-à-vis pure PU is explained from the absence of hard segment in modified graphene containing system as agglomerated hard

segments act as extra reinforcing agents for polymeric systems. However, ethylene diamine and hexyl diamine functionalized graphene containing nanocomposites exhibit excellent toughness as compared to pure PU presumably of stress transfer mechanism in presence of enhanced interfacial interactions along with homogenous dispersion of modified graphene in polymer matrix [Shah et al. (2005)]. However, reduced modulus and enhanced toughness provide the extra flexibility in nanocomposites (PUG-E and PUG-H) and, hence, tune the mechanical properties induced by the chemical tagging of graphene with appropriate length of modifier with polyurethane main chain.

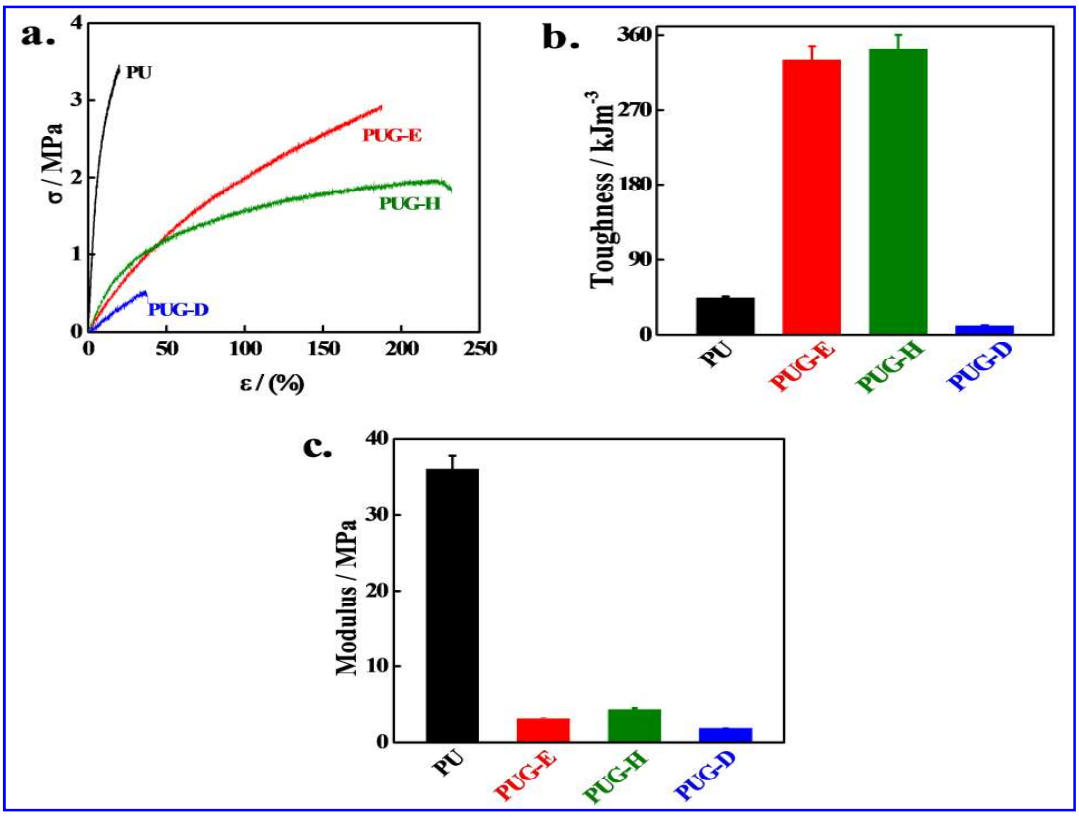


**Figure 5.7:** Mechanical response of the PU and its indicated nanocomposites. **(a)** stress- strain curve of pure PU and its indicated nanocomposites **(b and c)** toughness and modulus values of pure PU and its indicated nanocomposites in the bar graph respectively.

**5.2.7 Functionalized graphene induced self-assembly**:

Layer by layer self-assembly of the polymer chains along with graphene sheets are demonstrated through XRD, SANS, AFM and POM in the length scale of nanometer, tens of nanometer, hundreds of nanometer and micron scale, respectively. Shoulders appear in the XRD patterns both for PU and its nanocomposites at ~6.2$^{o}$, corresponding to the d-spacing of 1.40 to1.46 nm, indicating the presence of nanostructure in the form of molecular sheet arising from the hydrogen bonded interactions with the neighboring molecules (Figure 5.8a). Subsequently, the appearance of small angle neutron scattering (SANS) shoulders at wavevector q ~ 0.39 nm$^{-1}$ with the characteristic length $\Lambda_c = (2\pi/q_m) \approx 14.2 - 16.0$ nm confirms the higher level of nanostructure with gradual decrease of $\Lambda_c$ with increasing spacer length of modifiers (Figure 5.8b). Lower characteristic length in nanocomposites (~14.2nm) indicate that lower number of molecular sheets are required to form bigger assembly observable through SANS in comparison to pure PU ($\Lambda_c$ =16.0nm). The characteristic lengths ($\Lambda_c$) are 16.1, 15.3, 14.7 and 14.2 nm for pure PU, PUG-E, PUG-H and PUG-D, respectively, and generally 9−11 numbers of molecular sheets are required for the formation of such type of nanostructure. The SANS patterns are best fitted with Ornstein-Zernike model (Equn. 1) and presented in (Figure 5.9)

$$I(q) = I(0) / 1+\xi^2 q^2 \quad \text{..... (1)}$$

Where, I(q) is the scattered intensity, I(0) is scattered intensity at zero wave vector, $\xi$ is the correlation length and q is the wavevector. The correlation lengths of pure PU, PUG-E, PUG-H and PUG-D are found to be 0.91, 2.14, 2.16 and 2.25nm, respectively.

Greater assembly of ~100 nm size is noticed through AFM micrographs and the strips becomes more prominent in nanocomposites as compared to pure PU indicating the close packing in presence of greater contrast functionalized graphene with the urethane linkages (Figure 5.8c). The average sizes of the assembly are 98, 120, 133 and 155nm for pure PU, PUG-E, PUG-H and PUG-D, respectively. Greatest assembly of micron scale is observed through optical images of PU and its nanocomposites with the dimension of ~2.2 ± 0.3μm (Figure 5.8d). Thus, layer by layer self-assembly phenomena which is responsible for the formation of such micron size inhomogeneities are evaluated through XRD (1.41nm), SANS (15nm), AFM (100-150nm) and POM (~2.5μm) in sequence and are being formed through extensive hydrogen bonding between the molecular sheet along with the graphene sheets. Structural properties of the polymer are highly influence through the nature of the filler. Layered silicate induced self assembly phenomenon has been reported earlier, where organically modified nanoclay strongly interact with polyurethane chains to form this extended self-assembly [Mishra et al. (2014)].

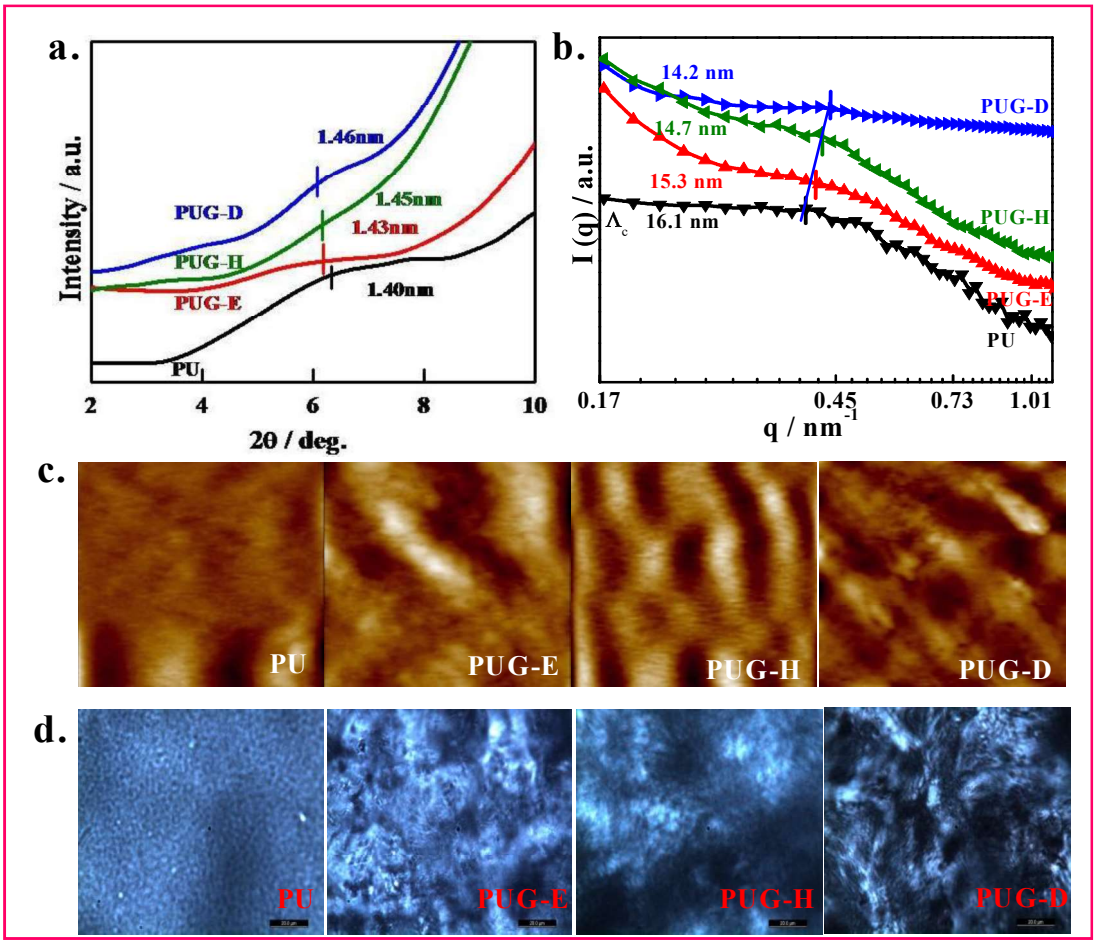


**Figure 5.8: (a)** X-ray diffraction patterns of the pure PU and its indicated nanocomposites. **(b)** SANS patterns of the PU and its indicated nanocomposites **(c)** AFM image of PU and its indicated nanocomposites (1μm×1μm) and **(d)** POM image of pure PU and its indicated nanocomposites. (Scale bar 20μm).

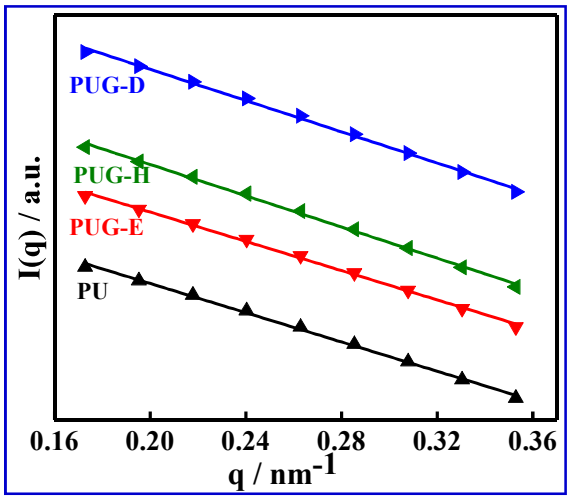


**Figure 5.9:** Ornstein- Zernike fitting for calculation of correlation length (ξ).

### 5.2.8 Sustained drug delivery – the effect of graphene tagging:

Sustain delivery of drug is very important to keep the drug concentration within the therapeutic window of the particular drug to obtain the best possible effect of drug. Standard curve was drawn after taking absorbance using 242nm in concentration range of 5-100 μg/ml and concentration of release drug was measured through UV-visible absorbance. Standard curve of drug is given in (Figure 5.10).

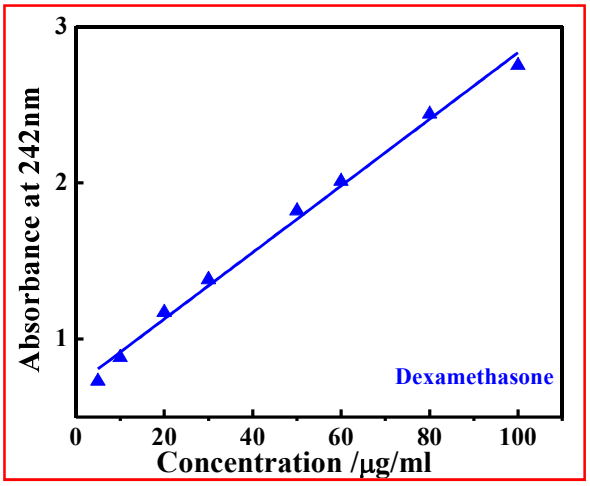


**Figure 5.10:** Standard curve of Dexamethasone standard stock solution (1mg/ml) drawn after taking absorbance using UV-visible spectrometer at 242 nm in the concentration range of 5-100 μg/ml.

In vitro drug release studies of anticancerous dexamethasone loaded drug in pure polymer and its nanocomposites are shown in (Figure 5.11a), taking phosphate buffer solution (pH ~7.4) as medium at 37 $^{o}$C**.** Initially, pure PU exhibits certain burst release (up to 10% only) followed by gradual release of drug while the drug release become sustained in nanocomposites significantly vis-à-vis pure PU. Further, drug release becomes increasingly sustained with increasing the length of spacer of the modifiers from ethylene diamine to dodecyl diamnie. Release kinetics of the loaded drug from

the pure polymer and its nanocomposits are best fitted ($r^2 \approx 0.99$) with Korsmeyer-Peppas model and are presented in (Figure 5.11b) leading to the exponent (n) value of 0.34, 0.46, 0.49 and 0.50 for pure PU, PUG-E, PUG-H and PUG-D, respectively, indicating the non-Fickian ($n \geq 0.45$) diffusion for nanocomposites as opposed to normal Fickian diffusion observed for pure PU. Sustained release in nanocomposite is primarily due to the presence of uniformly distributed two-dimensional graphene sheets which restrict the diffusion of drug molecule by creating the tortuous path while increasing interaction, as evident from spectroscopic measurements, with longer spacer length sustain the drug release even superior manner (Figure 5.11c). There are three major pathways namely, i) penetrations of liquids into matrix, ii) dissolution of drug, and, iii) diffusion process play importance roles in drug delivery and any of these three process may act as a rate determining steps [Singh et al. (2012)]. In this case, a change in diffusion process is observed from Fickian in pure polymer to non-Fickian in nanocomposites and might be considered as the rate determining step. Further, the exponent values gradually increase with longer spacer dimension to functionalize graphene help sustained release of drug. Graphene or its derivatives are frequently used as a drug carrier due to its high surface area along with different functionalities attached which facilitates the drug binding, as well as the biocompatible nature [Goenka et al. (2014)]. Further, Drug delivery process is highly influenced by the nature of the chain extender and filler used into the polymer matrix [Mishra et al. (2012)]. It is observed that the rate of diffusion of incorporated drug from the nanocomposites get decreased with respect to the pure polymer as the length of the diamine modifier increased for graphene modification. This is worth mentioning that

delayed diffusion in nanocomposites is partly responsible for the greater self-assembly patterns facilitated by the domain structure as clearly observed in the POM, AFM and SANS measurements. These domains structure also hindered the release rate of drug from the matrix.

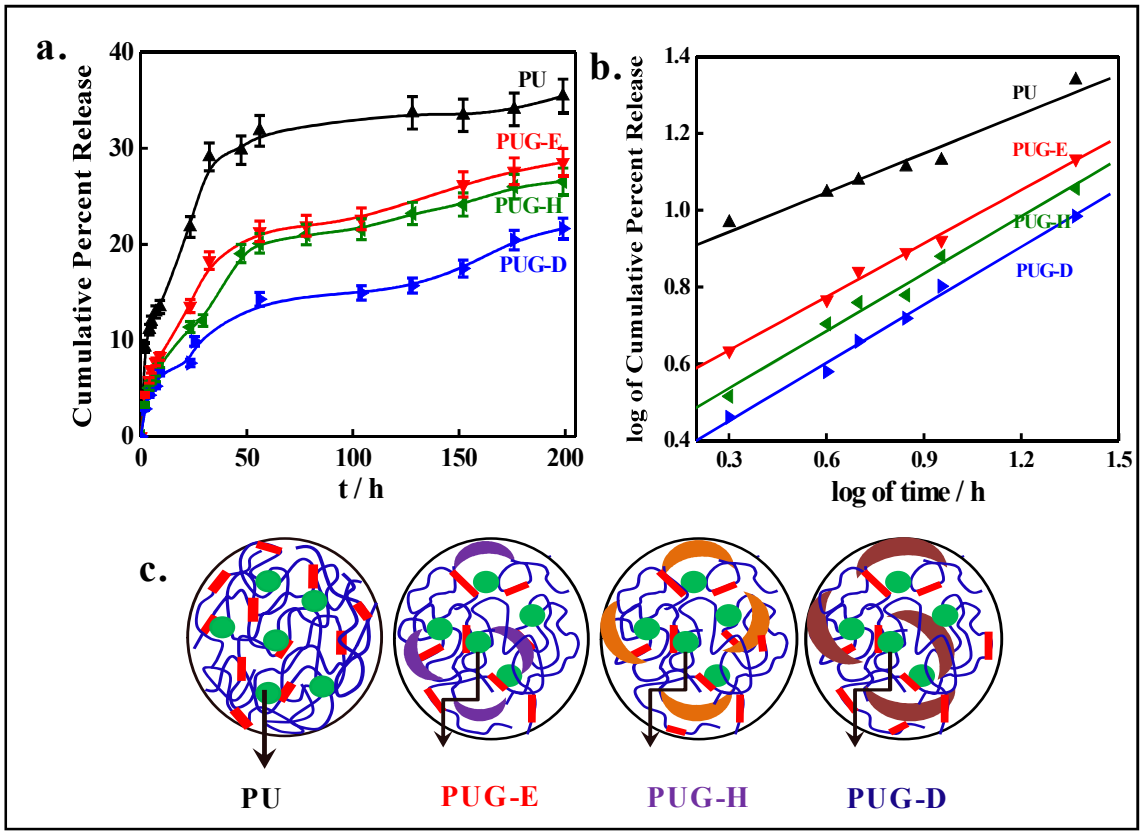


**Figure 5.11: (a)** Sustained drug release profile of pure PU and its indicated nanocomposites. **(b)** Korsmeyer- Peppas model for mechanism of drug release in PU and its indicated nanocomposites and **(c)** Schematic model of drug release kinetics. The green spheres and disc represents the drug molecule and modified graphene respectively. Disc size increase with increasing the modifier chain length and arrow represents the probable path for drug release through the matrix.

**5.2.9 Biological studies - cell viability and adhesion:**

Viability of cells over any material indicates the biocompatibility of that material. Viability of human breast cancer cells (MDA-MB231) on the surface of pure PU and its indicated nanocomposites has been studies through MTT assay and has been presented in (Figure 5.12a), at different time intervals**.** Cell viability increases with time both for pure PU and nanocomposites and interestingly the nanocomposites exhibit higher cell viability as compared to pure PU indicating better biocompatibility of nanocomposites vis-à-vis pure PU. Amongst the nanocomposites, graphene modified with ethylene diamine (PUG-E) shows higher cell viability as also evident from the cell morphology (Figure 5.12b) as observed from the fluorescence image of human breast cancer cells MDA-MB231of pure PU and its nanocomposites using acridine orange and ethydium bromide dyes. This is worthy to mention that cell health is the best using PUG-E as the media and somehow squeezed cell morphology is noticed in other cases. Graphene or functionalized graphene are widely used as scaffolds material for cell proliferation and differentiation of the stem cell to evaluate its biocompatible nature [Zanello et al. (2006)]. Graphene prepared through CVD technique did not show any toxic behavior for human osteoblasts and hMSCs [Kalbacova et al. (2010)]. Amine functionalized graphene did not alter the cell viability of the human monocyte cell line after 24h even at higher concentration (2-20 μg / mL) [Singh et al. (2012)]. Chowdhury et al. reported that oxidized graphene nanoribbons (O-GNR) exhibit different level of cytotoxicity with various cells. Enhancement in the cell viability was observed in 7-breast cancer cells (MCF7) and mouse fibroblast cells (3T3) while a decrease in viability was observed in HeLa cells[Chowdhury et al. (2013)].

Cell adhesion experiment indicates the possible use of the biocompatible materials as transplant or how the cells grow and adhered onto a support material. Cellular behavior such as cell adhesion, proliferation and differentiations are highly affected by the surface modification, surface charge, size, structural defect and surface wettability [Yang et al. (2013)]. Adhesion behavior of the human breast cancer cells MDA-MB-231 cell on the surface of pure PU and its nanocomposites are shown in (Figure 5.12c). Live cells are properly attached on the polymer/nanocomposites surfaces whereas the dead cells remain floated on the surface, though very less in number. Nanocomposites exhibit better cell adhesion as compared to pure polymer. Better cell adhesion in PUG-E with respect to pure polymer is better understood from the more hydrophilic nature of nanocomposite as evident from the slight lower contact angle of nanocomposite as compared to pure PU. Contact angle values are 78.3, 76.9, 78.2 and 78.3$^{o}$ for pure PU, PUG-E, PUG-H and PUG-D, respectively. Myoblast cell growth on modified graphene oxide is reported to have better adhesion and differentiation cellular behavior with respect to cell cultured on glass substrate [Ku et al. (2013)]. Differentiations of the hMSCs into chondrocytes on the surface of the graphene foam were also observed by Andy Nieto [Nieto et al. (2015)]. However, nanocomposites especially PUG-E exhibits better biocompatibility vis-à-vis pure PU. In brief, surface chemistry of the nanomaterial play an important role in biocompatibility and hence different functionalization of graphene exhibits the different varying level of cytotoxicity.

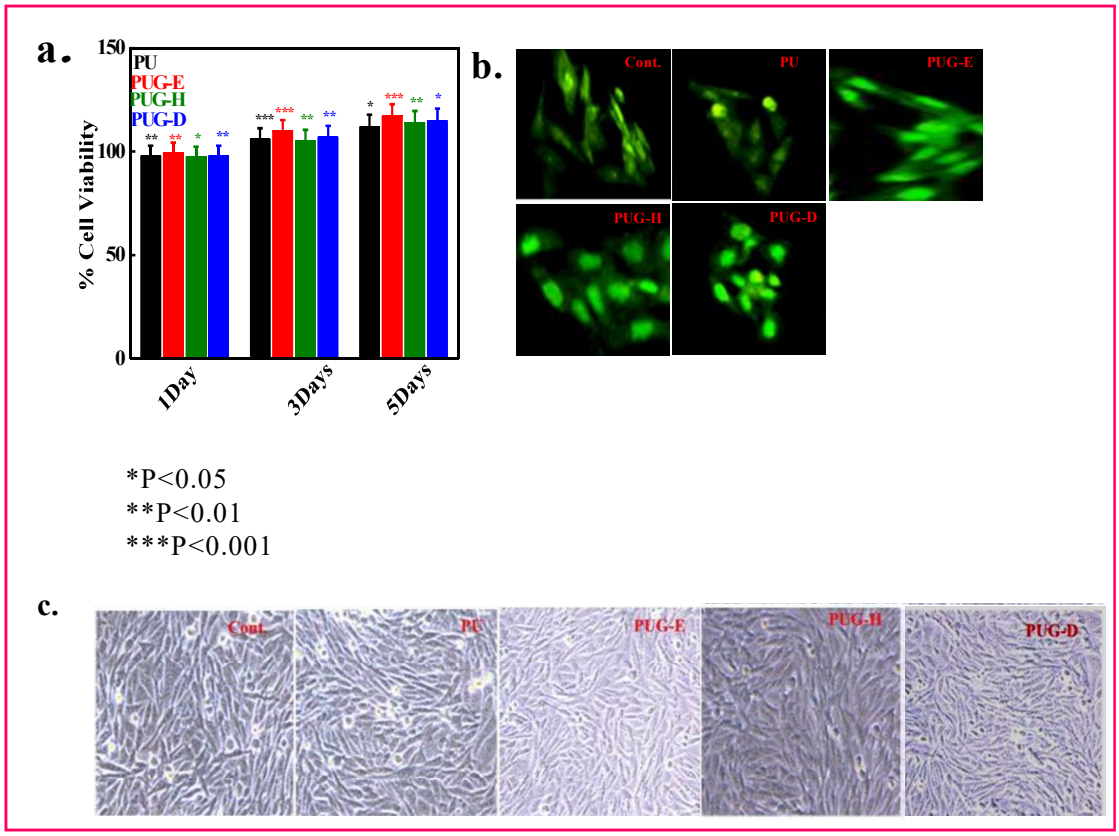


**Figure 5.12:** Biological behavior of pure PU and its indicated nanocomposites **(a)** Cell viability of pure PU and its indicated nanocomposites with time interval of 1, 3 and 5 days **(b)** Fluorescence microscopic image of PU and its indicated nanocomposites after 1 day of cell proliferation (Mag: 20×) and **(c)** Cell adhesion on pure PU and its indicated nanocomposites after 1day.

### 5.2.10 Intracellular reactive oxygen (ROS) contents and mitotracker analysis:

Biocompatible nature of PU and its nanocomposites are also verified and compared through the generation of intracellular reactive oxygen contents with respect to control and are presented in (Figure 5.13a). 2,7 Dichlorodihydrofluorescein diacetate (DCFH-DA) a non polar dye was used to measured the ROS content which converts into polar non fluorescent DCFH by cellular esterase. This non fluorescence component changes to highly fluorescence DCF through oxidation of the ROS and other peroxides [Rastogi

et al. (2010)]. Nanocomposites generate slight lower ROS species as compared to pure PU indicating better biocompatible nature of the nanocomposites. ROS values are 10.87, 10.73, 10.82 and 10.91for pure PU, PUG-E, PUG-H and PUG-D, respectively. Generation of ROS occurs when the cells are under stress conditions. There is no enhancement in the ROS level in nanocomposites as compared to pure PU which further support the biocompatible nature of the nanocomposites. Induced generation of ROS occurs when rat macrophages (NR8383) and human A549 lung cells are treated with SWCNTs and MWCNTs, however, no considerable toxicity observed on cell viability with incubation of cells along with these materials [Pulskamp et al. (2007)].

Mitotracker analysis is another special technique to investigate the biocompatible nature of materials. Polarization or depolarization behavior of the mitochondria around the nucleus indicates the nature of the materials whether they are biocompatible or not. Scattered nature of the mitochondria indicates the toxic affect of the materials however polarized behavior suggests the biocompatible nature. Mitotracker responses on pure PU and its nanocomposites using mitotracker red and DAPI dye are presented in (Figure 5.13b). Cells seeded onto the nanocomposites film exhibit more polarized behavior than pure polymer suggesting better biocompatible nature of the nanocomposites and amongst the nanocomposites, PUG-E shows best result with clear polarized images of mitochondria. Inhibitions of metastasis of MDA-MB-231 cells have been reported Zhou et al. in presence of graphene by the reduction of ATP production by decreasing the electron transport activity [Zhou et al. (2014)].

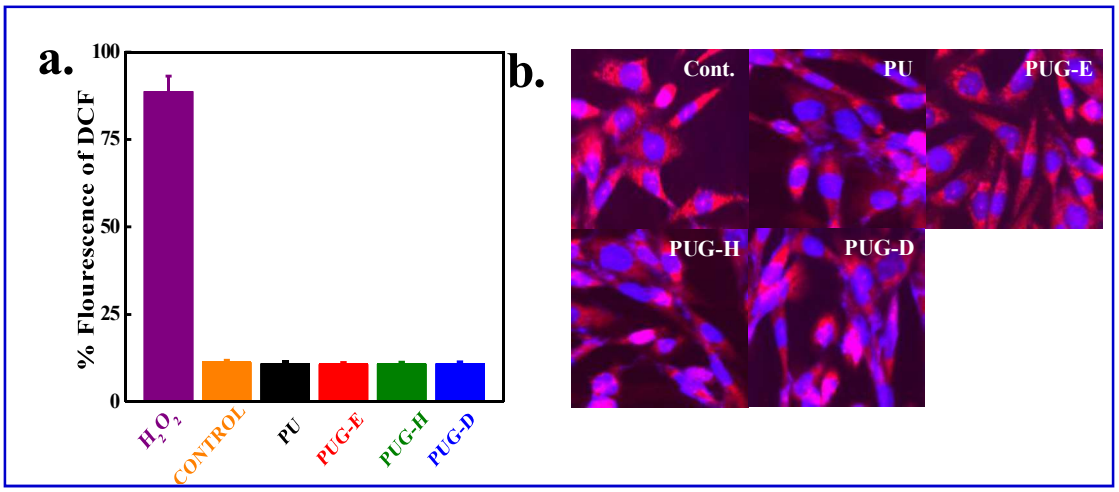


**Figure 5.13: (a)** Formation of the ROS in MDA-MB-231 cells in presence of pure PU and its indicated nanocomposites after 24 h of incubation. **(b)** Mitotracker staining with DAPI of MDA-MB-231 cells on PU and its indicated nanocomposites.

## 5.3 Conclusion:

Properties of the nanocomposites are highly influence through the nature of the modified graphene. Modification of the graphene was confirmed through the FTIR, UV-visible and XRD measurements. Surafce functionalization of the graphene oxide by the various diamine moiety leads to improve the properties of the nanocomposites in term of interaction, thermal and mechanical properties. Induced self-assembly through the modified graphene was facilitated in nanocomposites. Control drug release is observed in nanocomposites with respect to the pure polymer and this is more prominent in nanocomposites having the larger alkyl modified chain. Biological toxicity of pure polymer and its nanocomposites were studies on human breast cancer cells MDA-MB-231. Nanocomposites exhibit the better cell viability, Fluorescence and adhesion properties. Biocompatibilities of the nanocomposites were also monitored in term of reactive oxygen species and mitotracker analysis. These results support the developed materials are biocompatible in nature and may use in control drug release and tissue engineering fields.